Transactions of the Royal Society of Edinburgh: Earth Sciences, **91**, 283–301, 2000

Relationships between granitoids and mineral deposits: three-dimensional modelling of the Variscan Limousin Province (NW French Massif Central)

C. Le Carlier de Veslud, M. Cuney, J. J. Royer, J. P. Floc'h, L. Améglio, P. Alexandrov, J. L. Vigneresse, P. Chèvremont and Y. Itard

ABSTRACT: Multidisciplinary three-dimensional modelling, involving geophysical, structural and geochemical data, has been used to study the relationships between magmatism, tectonics, fluid circulation and mineralisation in the northern Limousin, and to provide P–T–Z–t paths constrained by the available dating. The ore deposit occurrence displays little spatial relationship with granites emplaced in the 360–320 Ma period, probably because the low global permeability and tectonic regime did not allowed vertical fluid exchanges to be established. In contrast, the change in the tectonic regime induced by the delamination of the lower lithosphere (320–300 Ma), and characterised by the passage to general extension, has played a major metallogenic role. However, the ore deposit processes appear to be specific to each metal. Most of the W–Sn deposits appear to be synchronous with rare metal granites emplacement, at *c.* 310 Ma, that allowed the focus of fluids of different origins towards the apex of plutons. In contrast, for Au and U, the whole mineralisation process covers several tens of millions of years. It is controlled by the regional tectonic evolution of the Limousin area during the same period, and especially by a rapid exhumation of the ductile crust which occurred in the 310–300 Ma period.

KEY WORDS: granite, Hercynian fluid circulations, ore deposits, thermal modelling, 3-D geometry

The French Massif Central (FMC) is characteristic of the whole Western European Variscan collision belt, in terms of types of geological terranes, granite types and ore deposits. Located in the NW of the FMC (Fig. 1), the Limousin has been a mining area, essentially for U, but also for Au, Sb, W, and F. At the present time, only U, Ba, Au and kaolin are still mined (Cathelineau *et al.* 1990; Cuney *et al.* 1990; Marignac & Cuney 1999).

U, Sn, W and Au mineralisations are spatially related to peraluminous leucogranites (Cuney *et al.* 1990). However, the formation of these different mineralisations spreads over a large time interval (about 50 Ma) after the intrusion of the granites. Therefore, several questions arise concerning the chronology and the role of geological events, the source of metal and the mechanisms which have led to the ore deposition. For that purpose, computer-aided three-dimensional modelling provides a common geometrical basis where all geological objects and data may be displayed. Such modelling appears to be a very efficient tool for checking the consistency between the different geological objects, and for studying the spatial and thermochronological relationships between geological structures and geochemical data (ore deposits, surface geochemistry). Under the auspices of the GéoFrance 3D national project '3D Mapping and Metallogeny of the French Massif Central', a three-dimensional reconstruction of the North Limousin crustal block (90 km × 90 km × 6 km) has been performed using the modelling software gOcad. The aim of this project was to understand better the genesis of mineralised districts at the end of the mid-European Variscan orogeny, during the 300±30 Ma time period.

1. Geological settings and available data

1.1. The tectono-magmatic history of the Limousin area

The West European Variscan belt is interpreted as resulting from a collision between two continental plates, Gondwana and Laurasia. However, the detailed history of this process remains controversial. In addition, a N–S chronological evolution of igneous events, as well as an E–W differentiation of the granite types, occur in the FMC (Marignac & Cuney 1999). Nevertheless, the following general chronology can be proposed for the Limousin area: (i) an Eo-Variscan stage (Silurian, 430–400 Ma), related to the closure of oceanic domains, which leads to the formation of high-pressure metamorphism recorded by eclogites (700 °C, 20 kbars); (ii) A Meso-Variscan stage (Devonian to early Carboniferous, 400–340 Ma), related to the continental collision and nappe stacking in Barrovian metamorphism conditions, culminating in anatexis in the eastern part of Limousin; the end of the nappe tectonics in Limousin is characterised by two main igneous events at *c.* 355 Ma: the so-called 'tonalitic line', consisting of a series of high and medium-K calc-alkaline diorites, tonalites and monzogranites, and huge laccoliths of peraluminous biotite ± cordierite granites (Guéret type); (iii) a Neo-Variscan stage (Visean to Namurian, 340–310 Ma), characterised in the Limousin by numerous strike-slip faults; the magmatism corresponds mainly to peraluminous two-mica laccolithic granites (Limousin type, intra to Late Carboniferous ages); (iv) a late-orogenic extensive stage may locally start in the middle Carboniferous, but more generally occurs from Late Carboniferous to Early Permian (Faure 1995, 320–280 Ma). This episode is particularly

Sedimentary units

Sedimentary cover

Visean sedimentary basin

Metamorphic units (from top to bottom)

Gartempe unit (Upper allochthon)

Upper Gneiss Unit (UGU)

Lower Gneiss Unit (LGU)

Relative Autochthon

Granitoïds

Quartz diorites: 1 Saint Barbant
2 Saulgond

Guéret-type: 3 Aureil, 4 Auriat, 5 La Glane, 6 Cieux-Vaulry, 7 Guéret, 8 Oradour-Saint Genest, 9 La Garde

Limousin-type: 10 Brâme, 11 Saint Sylvestre, 12 Saint Goussaud, 13 Blond, 14 Saint Sulpice, 15 Western Marche, 16 Crozant, 17 Cognac, 18 Central Marche, 19 Chabanne belt, 20 Millevaches

Main thrust

Migmatites

Fault

Figure 1 Regional geological map of the modelled area: main thrusts, regional faults and granitic massifs are shown; extended Lambert II coordinates system is indicated on the margin of the map.

Table 1 Isotopic dating of the main granitic massifs involved in this study.

Granitoid	Typology	Age (Ma)	Method	Reference
Aureil	Guéret-type	346 ± 14	Rb/Sr	Duthou 1978
Auriat	Guéret-type	324 ± 1	U/Pb on zircon	Gebauer *et al.* 1981
Blond	Limousin-type	319 ± 7	U/Pb on zircon	Alexandrov *et al.* 2000
Brame-Saint Sylvestre complex	Limousin-type	324 ± 4	U/Pb on zircon and monazite	Holliger *et al.* 1986
Cieux-Vaulry	Guéret-type	352 ± 12	Rb/Sr	Duthou 1978
Cognac	Limousin-type	308 ± 11	Rb/Sr	Duthou *et al.* 1984
Crozant	Limousin-type	312 ± 20	Rb/Sr	Rolin & Quénardel 1982
Guéret	Guéret-type	356 ± 10	Rb/Sr	Berthier *et al.* 1979

intense in the SE of the FMC and is associated with the development of migmatitic domes and coal basins. In the Limousin, these types of structures have not been observed. The last stage is synchronous with the granulite-facies metamorphism of the lower crust during the Late Carboniferous (Pin & Vielzeuf 1983). The associated thermal anomaly and potential fluid circulations reflect the thermal relaxation of a thickened crust. In the Limousin, the corresponding Late Carboniferous magmatism is limited to the intrusion of small but highly specialised granites that commonly are located near fault zones.

1.2 Available data used for 3-D modelling

Data used in the modelling are: (i) most recent 1/50,000 geological and structural maps of the area (including magmatic, ductile and brittle structures); (ii) ten interpretative vertical geological cross-sections; (iii) three-dimensional models of granite shapes derived from the inversion of a systematic gravimetric data survey (more than 1 point/km^2); (iv) age determinations mainly on granites (Table 1); and (v) whole rock and regional stream sediment geochemistry, mineral occurrences and ore deposits from the BRGM databank. Time, temperature and pressure constraints were provided by thermobarometric, geochronological and thermochronological data from the literature. All the coordinates are expressed in the Extended Lambert II system, a metric rectangular system based on a conformal conic projection, centred on the Paris meridian and covering all of France.

The inversion of gravity data provides a first-order representation of the three-dimensional shape of the plutons. However, this process is very sensitive to the density contrast between granite and surrounding rocks. Therefore, it appears to be reliable for Limousin-type granite, presenting a relatively large density contrast, with an estimated uncertainty of less than 15 % (Ameglio *et al.* 1997). In contrast, the Guéret-type granites display a more variable and globally smaller contrast (Laurent 1989), leading to a greater uncertainty in the determination of their shape. Table 2 summarises the data used to build the three-dimensional shape of the granites.

1.3 The construction of the 3-D model

The geometrical modelling was performed using the gOcad three-dimensional visualisation and modelling software, specifically adapted to geosciences applications (ASGA 1999, Mallet 1997). The creation of a geologically relevant three-dimensional model in complex regions is a difficult task. If in the northern Limousin the surface geology is relatively well known, the lack of accurate data at depth (deep boreholes, seismic data) may induce a wide range of interpretations. It is therefore important to constrain these interpretations as much as possible by using field data. Thus, the construction of the three-dimensional model is based on three stages, involving three kinds of objects (Fig. 2): (i) the first step consists of the introduction of data, that represents partial and local information indicating the location of geological structures. For example, those data may come from boreholes (isolated points with dips), from structural maps (two-dimensional lines with dips, describing the intersection of the structures with the topographic surface), or from gravimetric data inversion (one-dimensional or two-dimensional point sets). Unfortunately, they are scarce, irregularly spaced, incomplete in the three-dimensional space, and in addition, they do not present the same level of uncertainties (Mallet 1997). Thus, (ii) the second stage (surfacic model) aims to link these data by using continuous or discontinuous triangulated surfaces, that represent the boundaries of geological objects (faults, contacts); and finally, (iii) in the third stage, a volumic model is derived from the surfacic model.

The surfacic model is one of the key-points of the work. The construction of surfaces from the data is performed using the Discrete Smooth Interpolator (Mallet 1992). This interpolator provides smooth surfaces respecting a wide set of potential constraints (Fig. 2). For example, *control point* constraints are used to build a surface from fuzzy data points or cross-section curves. In addition, *control slope* constraints allow the shape of geological interfaces (faults or contacts) to respect structural field data, such as magmatic or tectonic fabrics as well as dips. The *on surface* constraint automatically imposes the best possible contact between the objects, for example a fault with a

Table 2 Data in depth used to build the shape of the granitic massifs.

Granitoid	Type of data	Reference
Western Marche	3-D gravimetric inversion	Vigneresse & Cuney 1994
Blond	3-D gravimetric inversion	Améglio *et al.* 1999
Crozant	2·5-D gravimetric inversion	Dumas *et al.* 1990
Guéret	2·5-D gravimetric inversion	Vasseur *et al.* 1990
	one borehole crossing the massif	Laurent 1989
Brame-Saint Sylvestre complex	3-D gravimetric inversion	Audrain *et al.* 1989
	2·5-D gravimetric inversion	Vasseur *et al.* 1990

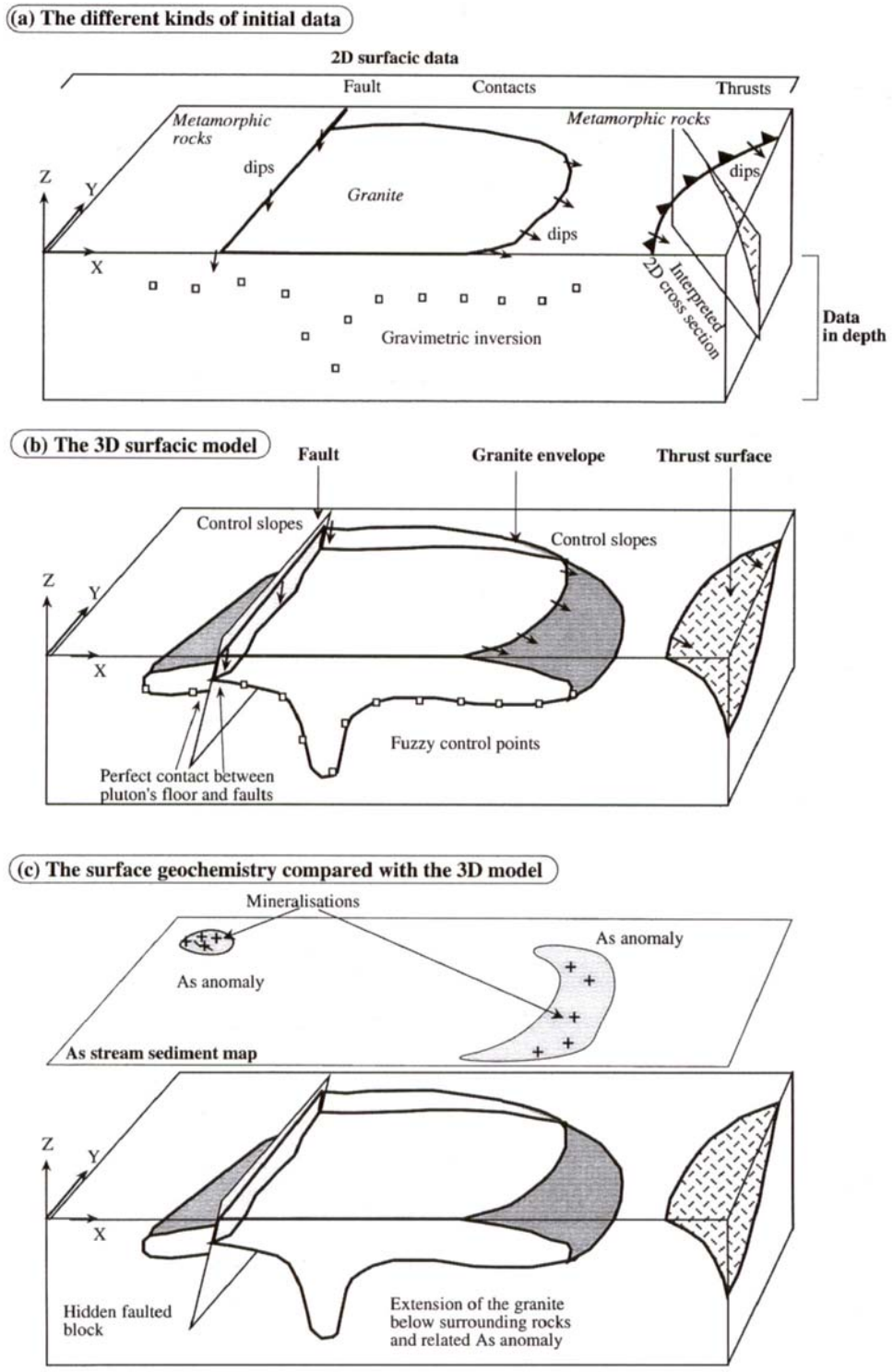

Figure 2 Synthetic chart describing the process used to build the three-dimensional model: (a) presentation of the different types of initial data; (b) these data are used as constraints of different types, in order to build a geometrically and geologically consistent surfacic model; (c) the surface geochemistry, including mineral occurrences and stream sediment data, is added to the three-dimensional model; this helps to investigate the relationships between ore deposits and geological structures.

horizon. Finally, the initial two-dimensional cross-sections were built assuming a two-dimensional thickness conservation. A *fuzzy constant thickness* constraint has here been used to extrapolate this assumption from two dimensions to three dimensions.

The topology of the surface may be automatically adapted to the variability of the data (for example by using curvature analysis or error estimates), allowing an increase of density of the mesh only where necessary. Boolean operators between surfaces (cuts, subtractions, extrusions, etc.) are used to simplify the construction of complex objects, particularly in the case of intrusions through other geological bodies. This wide set of construction tools allows an almost automatic surfacic modelling, ensuring the consistency of geological and geometrical relationships between objects, in agreement with the geologist's point of view (Mallet 1997).

Finally, a volumic model is used to deduce automatically the partition of the space into regions from the surfacic model. These volumic models may be used to compute the volumes of intrusions or of faulted zones, which constitute several first-order parameters for studying the impact of such intrusions on the surrounding rocks (contact metamorphism and fluid motion). These volumic models are also used to affect physical properties (permeability or thermal conductivity for example) in a mesh. These types of information are used as an input to perform modelling of heat and mass transfers on the three-dimensional transient finite element software Thermass (Gérard 1997).

2. Structure of granite complexes

2.1 The nappe pile

Four main lithostructural metamorphic units, separated by low dip thrust contacts, are present in the Limousin area (Fig. 1) (Ledru *et al.* 1989): (i) the Upper Allochthon, representing low-grade Palaeozoic units (Gartempe unit in Limousin); (ii) the Middle Allochthon (Upper Gneiss Unit or UGU in Limousin), a high-grade unit, characterised by numerous high pressure relicts, and made up of basic metagreywackes, and acid and basic meta-igneous rocks called 'leptyno-amphibolitic complex', with ophiolitic units occurring at its base; (iii) the Lower Allochthon (Lower Gneiss Unit or LGU in Limousin), mainly consisting of acid metagreywackes and acid metagranites, dated from Early Cambrian to Ordovocian; (iv) the Para Autochthon, mainly made up of micaschists, metagreywackes and rare orthogneisses.

The main metamorphic gneissic units are organised in large but complex decakilometric-length antiforms, which were formed 60 Ma after the nappe stacking (at *c.* 320 Ma, Autran & Guillot 1975), probably in response to large leucogranitic intrusion emplacement (Lespinasse *et al.* 1986; Faure & Pons 1991).

The evolution of the Meso-Variscan shear tectonics remains controversial; however, recent studies on the South Limousin area (Roig & Faure 2000) suggest a polyphase shear tectonics for that period, corresponding to two different thrusting events. The first one thrust the UGU over the LGU during the Middle Devonian period (*c.* 380 Ma). During the Late Devonian (*c.* 360 Ma), a second event thrust the UGU and the LGU onto the Para-Autochthon Unit, and the Upper Allochthon onto the gneissic units.

2.2 The main types of granitoids

Two main types of granitoids were produced in the FMC during the Variscan orogeny: (i) medium- and high-K calc-alkaline and (ii) peraluminous granitoids (Stussi 1985). In the Limousin, the first type was mainly emplaced during the Early Carboniferous and middle Visean, at *c.* 355 Ma (Bertrand *et al.* 2001). In the Northern Limousin, this type mainly corresponds to quartz-diorites (Fig. 1). These diorites appear as kilometric-sized bodies, concordant with surrounding rocks (mainly UGU). They do not seem to be deeply rooted (Peiffer 1986). However, in the Vienne region (40 km to the NW), interpretation of geophysical surveys suggests a much larger thickness (< 5 km) for this type of granitoid (Virlojeux *et al.* 1999). These granitoids are not associated with any significant mineralisation and, thus, will not be considered further in the present paper.

The peraluminous granites represent more than 80% of the granites in the Limousin. Two different types of peraluminous granites have been discriminated in the Limousin (Turpin *et al.* 1990a; Stussi & Cuney 1993; Cuney & Stussi 1999) (Fig. 1): (i) biotite ± cordierite granites (Guéret-type) emplaced mainly at 350 ± 10 Ma (with the exception of the Auriat massif, see Table 1), and (ii) two-mica leucogranites (Limousin-type) emplaced at 320 ± 15 Ma. According to Turpin *et al.* (1990a), the isotopic data suggest a mixed origin for Guéret-type granites, involving partial melting of peraluminous metasedimentary rocks and basic metaigneous rocks. In contrast, the Limousin-type granites would have been generated by pure crustal partial melting, involving extensively Late Precambrian-Early Palaeozoic granites. The source rocks of these peraluminous granites could be found in the metamorphic pile of the Limousin.

Finally, several small, highly peraluminous Rare Metal Granite (RMG) intrusions, rich in Sn Ta, W and U, were emplaced during the Westphalian (*c.* 310 Ma, Marignac & Cuney 1999), inside or in the vicinity of Limousin-type leucogranites. They were generally considered as highly differentiated magmas deriving by fractionation from the spatially associated leucogranites (Pollard 1989), but recent studies suggest that they may derive from an independent magma (Cuney *et al.* 1994). In the Limousin area, the RMG appear either as pegmatitic, microgranitic to rhyolitic dykes, or as small granitic cupolas. Their high Li, F and P contents, decreasing the viscosity of the silicate melts, allow a rapid upward injection of the magma through dykes. They are associated mainly with Sn + W ± U mineralisation, but also with Li, Be and Ta mineralisation (Marignac & Cuney 1999). The available isotopic dating of all these granites is presented in Table 1.

2.3 Geometry of intrusions

The studies of the geological maps, the regional shear zones (Lespinasse *et al.* 1986; Guineberteau *et al.* 1989) and of the geochemical data (Turpin *et al.* 1990a, Stussi & Cuney 1993) indicate that the peraluminous granites are organised mainly as four major complexes (Fig. 1). The Brame–Saint Sylvestre complex, located in the centre of an antiform structure, consists exclusively of Limousin-type granites. Three other complexes (Guéret, Western Marche and Blond–Cieux–Vaulry) emplaced close to the UGU/LGU thrust plane, involve Guéret-type granites intruded by Limousin-type granites.

Guéret-type granites appear as large but thin (about 1 to 2 km on average) laccoliths, resulting from a syntectonic magma emplacement along the main regional thrusting plane between the UGU and LGU. The Guéret-type granite foliations are mainly horizontal and concordant with surrounding gneiss, reflecting a common history during the end of the nappe construction, at *c.* 355 Ma. Along some restricted bands, the foliation is vertical and associated with a greater thickness of the granite slab, or with shear zones active during the emplacement of these granites (Guineberteau *et al.* 1989). This type of granitoid is not associated with any

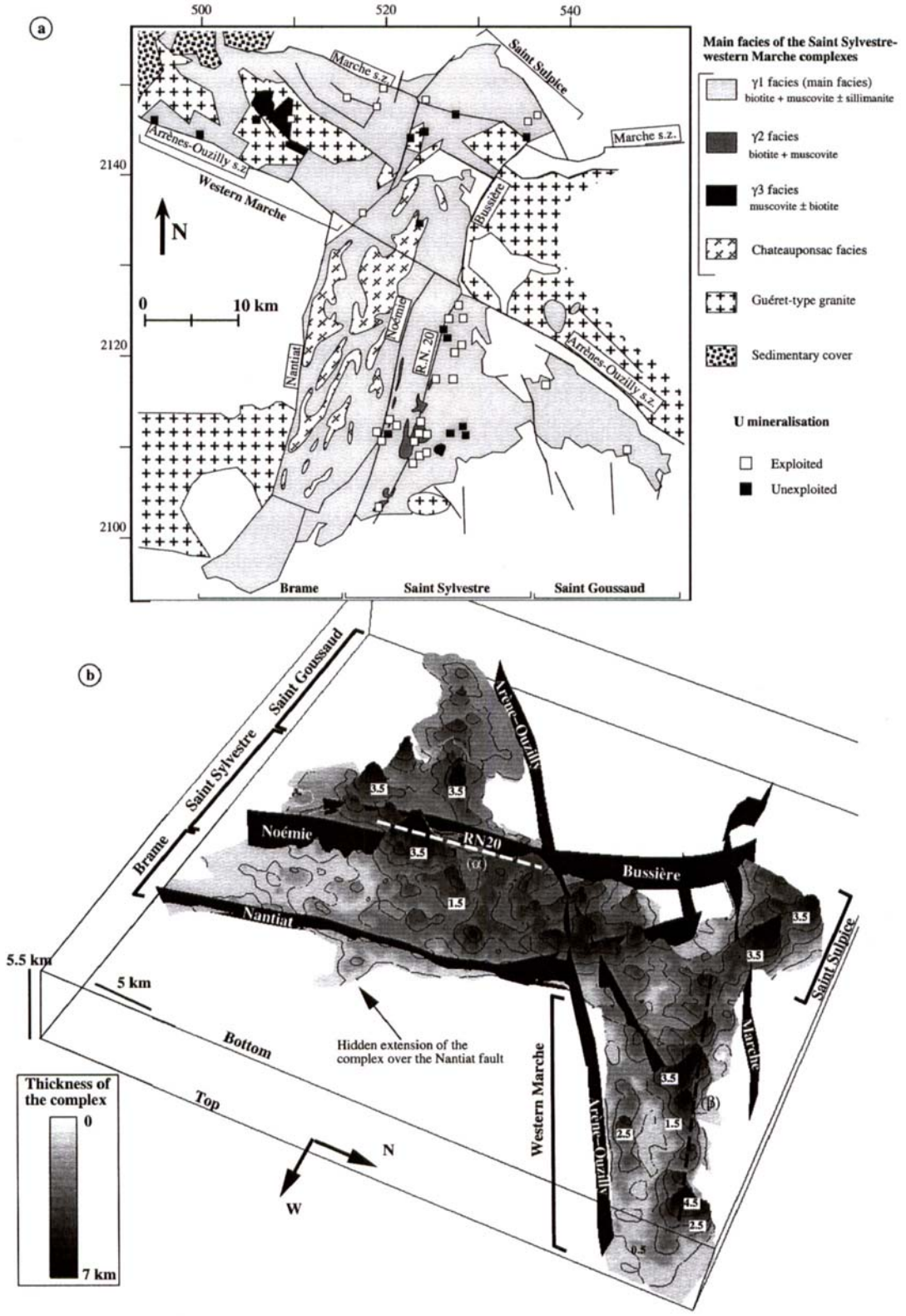

Figure 3 Saint-Sylvestre–Western Marche complex and U deposits: (a) top view of the different facies outcropping in the complex, superimposed with U ore deposits; extended Lambert II coordinates system indicated; (b) three-dimensional simplified view from the bottom, without any scale exaggeration; the main faults bounding the complex are shown; the thickness of the massifs is mapped in grey scale, in addition to isodepth lines (1 km interval); two alignments of deep zones, oriented N20 and N110, are highlighted; each of these alignments corresponds to the outcrop of late $\gamma 2$ or $\gamma 3$ facies, associated with several economic to subeconomic U deposits (see Fig. 3a).

mineralisation. Some U, W and Au anomalies or deposits are generally related to numerous small, late leucogranitic intrusions, rarely occurring as cupolas inside the massifs (Laurent 1989). The Auriat Guéret-type granite, atypically emplaced more than 25 Ma after the other Guéret-type granites (Table 1), displays structural characteristics similar to those of Limousin-type (see below).

The Limousin-type granites are mainly emplaced below Guéret-type granites (as in the Brame–Saint Sylvestre complex) or are intrusive in these granites (as in the Western Marche or Blond massifs). They are concordant to discordant with surrounding metamorphic rocks. For the Namurian Limousin-type granitoids (e.g. the Brame–Saint Sylvestre–Western Marche complex), the shape of the intrusion corresponds to relatively thin (1–3 km thick) but large (up to 50 km wide) laccoliths, controlled by the regional tectonics. For the late Limousin-type intrusions, (e.g. Aigurande plateau plutons), the corresponding shape is more elliptical (Faure 1995) because the magma dynamics were strong enough to counterbalance the effects of the regional tectonics.

In the Saint Sylvestre–Western Marche complex, the petrogeochemical studies indicate a symmetrical evolution with respect to the Brame unit. The Saint Sylvestre–Saint Goussaud blocks toward the E, and the Western Marche toward the W, are enriched in incompatible elements. These features, concordant with structural studies of the faults limiting the complex, highlight a horst structure. The Brame unit is the most uplifted block. The Saint Sylvestre–Saint Goussaud blocks toward the E, and the Western Marche toward the W, represent down-faulted more apical parts. The final horst structure was formed during a brittle extensive phase that has mainly reactivated previous magmatic and locally ductile shear zones.

For most of these granites, magmatic structures are shallowly dipping and magmatic lineation is constantly NW–SE. Vertical magmatic structures occur along, or close to regional ductile shear zones, either bounding these granites or separating Guéret-type from Limousin-type granites. Vertical magmatic structures also occur where deeper roots were defined by three-dimensional inversion of gravimetric data, commonly reaching a depth of 5 to 7 km. For example, in the Brame–Saint Sylvestre complex (Fig. 3b), deeper rooted zones down to 6 km, correlated with vertical lineations, occur along a major N20 lineament (Audrain *et al.* 1989), inside which numerous highly fractionated granites ($\gamma 2$ and $\gamma 3$ facies, also enriched in rare metals (Cuney *et al.* 1990), see Fig. 3a) were emplaced. Cuney *et al.* (1990) interpret this lineament as a major crustal scale structure that has collected magmas throughout the emplacement of this complex. Similarly, in the case of the Western Marche complex (Fig. 3b), a N110 oriented, 3–5 km-deep zone (Vigneresse & Cuney 1994) is correlated with highly fractionated granite ($\gamma 3$ facies (Cuney *et al.* 1990), see Fig. 3a) and with a major mylonitic zone located inside the complex (Guineberteau *et al.* 1989). We show later that these relations are of major importance for U metallogenesis in these granites.

The geometrical characterisation of RMG and their relationships with Limousin-type granites are difficult to establish, due to their small size. Three-dimensional information provided by gravimetric inversion locally helps to constrain such relations. For example, four RMG dykes or veins have been located inside the Blond massif or in its vicinity (Cuney *et al.* 1999). The Blond Limousin-type granite displays four discontinuous facies, followed by Li-muscovite and topaz leucogranitic intrusions occurring to the NW of the main body (Fig. 4a) (Barbier 1967; Raimbault 1998). The inversion of gravimetric data (Ameglio *et al.* 1999) shows that this massif appears as a sill. To the SE, a deepening of the pluton's floor, reaching a 2–4 km thickness, is orientated N60 (Fig. 4b and c). To the N, the massif displays a thin laccolithic shape, with several deep zones underneath the outcrop of topaz leucogranites (Fig. 4c). These features may be interpreted as the roots of the more differentiated facies. Similarly, W of the Oradour fault, a deep zone reaching a depth of 3 km is correlated with the Brillac RMG dykes, and could correspond to the root of this intrusion.

3. Implications for mineralisation processes

3.1 Main ore deposit formation conditions

The conditions of formation of the different ore deposits in the FMC during the Variscan orogeny have been studied in detail (Cathelineau *et al.* 1990; Cuney *et al.* 1990; Marignac & Cuney 1999).

Some non-economic tin deposits occur in the Limousin area, most of which are located inside granites, close to Sn-rich facies (Cuney *et al.* 1990). Similarly, Be deposits are associated with pegmatitic intrusions.

Quartz–wolframite stockworks represent the most common type of W deposits in the FMC. They are located close to the contact with leucogranites or Rare Metal Granites, either in enclosing metamorphic rocks as stockworks or inside the granites as greisens. Most of the deposits were formed at pressures around 1 kbar (Aissa *et al.* 1987), with the exception of the Puy-les-Vignes hydrothermal breccia, where a pressure of $2{\cdot}5 \pm 0{\cdot}5$ kbar was determined (Alikouss 1993). Fluid inclusion studies suggest a common pattern for the fluid circulations: high temperature (about 500 °C) aquo-carbonic fluids, diluted by low saline fluids, resulting in W deposition at temperatures *c.* 350–400 °C. The high temperature fluids are probably of metamorphic derivation (Marignac & Cuney 1999). A Namurian–Early Stephanian age (315–300 Ma) is proposed for these deposits, in conjunction with granites generated during the Sudetian phase.

Gold deposits in the Northern Limousin are mainly located in conjunction with long-lived shear zones or in the vicinity of the Limousin-type granites, strongly correlated with As anomalies (Fig. 5a, b). Mineralogical and fluid inclusion studies (Boiron *et al.* 1989, Bouchot *et al.* 1989, Touray *et al.* 1989) suggest two episodes of fluid circulation: (i) a high-temperature episode (350–400 °C, 1–2 kbar), during which fluids are mainly of metamorphic derivation, associated with arsenopyrite deposition; (ii) a low-temperature episode (150–200 °C, 0·3–0·5 kbar), with low saline meteoric fluids, associated with the main Au deposition. The Au deposition was caused by the conjunction of two favourable conditions (Cathelineau *et al.* 1990): (i) the presence of quartz sulphide-arsenide bearing veins, formed during ductile deformation, to which the first type of fluids could be related. (Bouchot *et al.* 1989; Nénert *et al.* 1997); and (ii) the brittle cataclasis of these quartz-sulphide veins, representing traps for ore deposition during the circulation of low-temperature fluids of meteoric derivation. The mineralisation is generally located in areas where first-order structures (regional ductile shear zones) are intersected by second-order structures (brittle deformation) in which ore deposition occurs (Eisenlohr *et al.* 1989). The age of deposition remains controversial; however, direct or indirect dating ranges from 310 Ma to 285 Ma (Marignac & Cuney 1999).

For U, a three-stage process was proposed by Cuney *et al.* 1990) and Scaillet *et al.* (1996a, b). (i) Firstly, an early pre-concentration stage resulted from magmatic enrichment in U during intrusion of $\gamma 2$ and $\gamma 3$ endogranites, emplaced along late magmatic shear zones. For example, in the Saint Sylvestre complex, those endogranites were emplaced along a N20 shear (Fig. 3a), between 324 Ma and 310 Ma (Scaillet *et al.* 1996a).

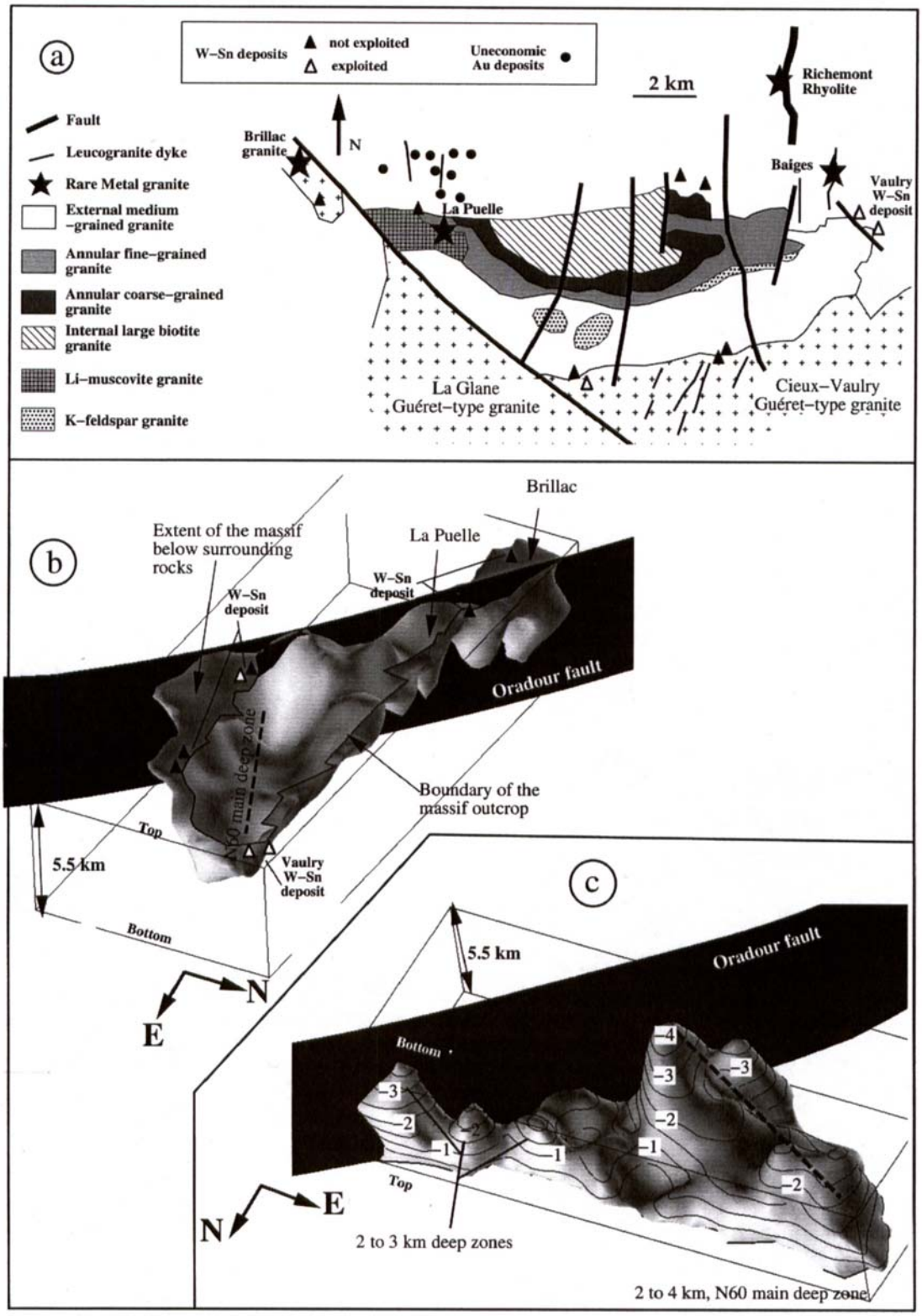

Figure 4 Blond massif: (a) different facies outcropping in the Blond massif after Raimbault (1998); (b) top view from the NE of the massif; to the S, the shape of the granite is low dipping and corresponds to an extension below the surrounding rocks; (c) bottom view from the NE of the deep zones of the granite; according to Améglio *et al.* (1999), the 2–4 km main deep zone is interpreted as the root of the massif; the three small deep zones located along the northern margin could correspond to the roots of late facies (isodepth in km).

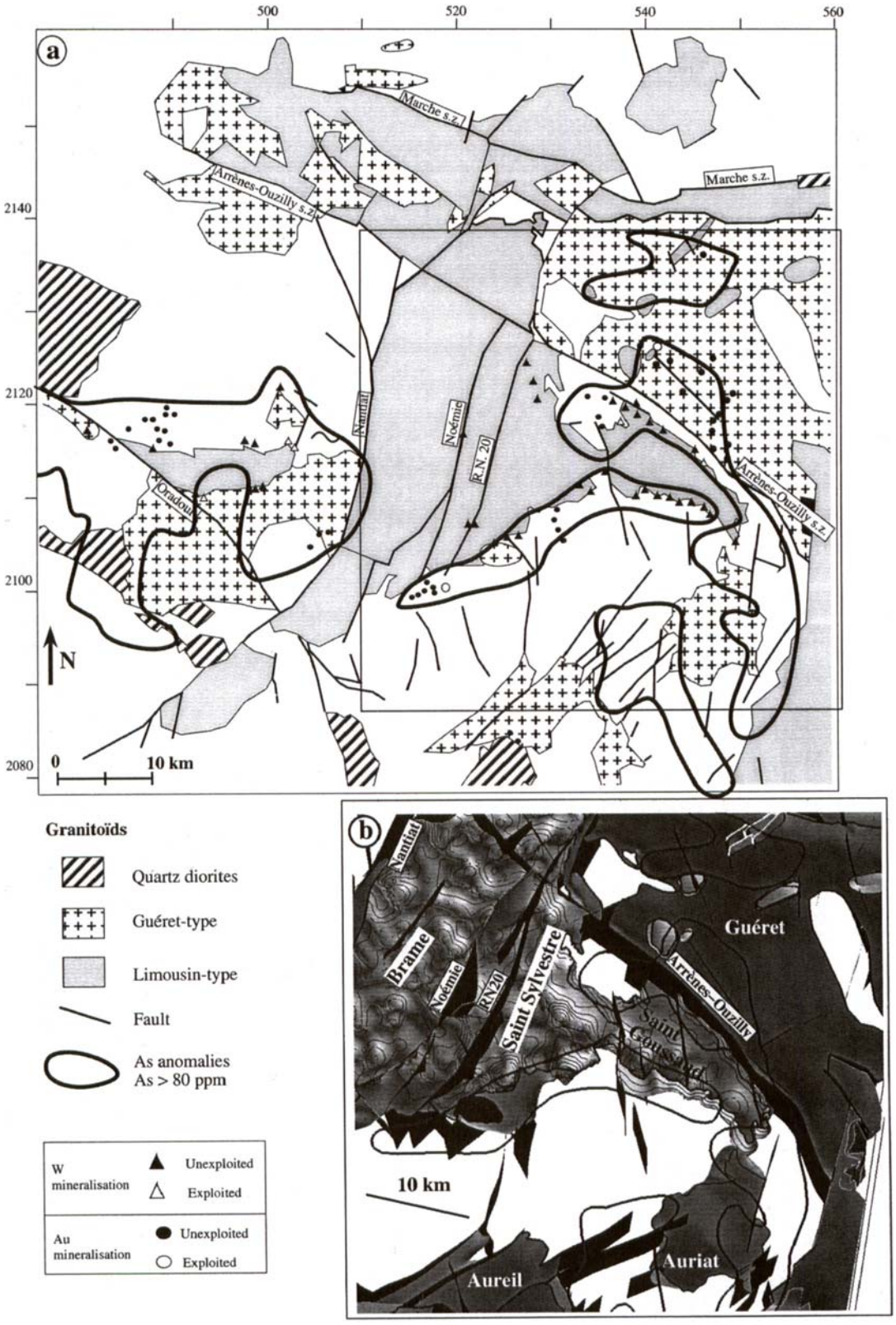

Figure 5 Au and W–Sn deposits: (a) simplified view of the main granitoids superimposed with As anomalies (As > 80 ppm) and both Au and W–Sn deposits; extended Lambert II coordinates system indicated; (b) three-dimensional view from the SE of the Saint-Sylvestre–Saint Goussaud massifs (no scale exaggeration) corresponding to the rectangular outline indicated in Figure 5a; the isoline interval is 0·5 km; the As anomalies are also displayed; they show a particular relationship with the periphery of Limousin-type granite, especially where this extends below surrounding rocks.

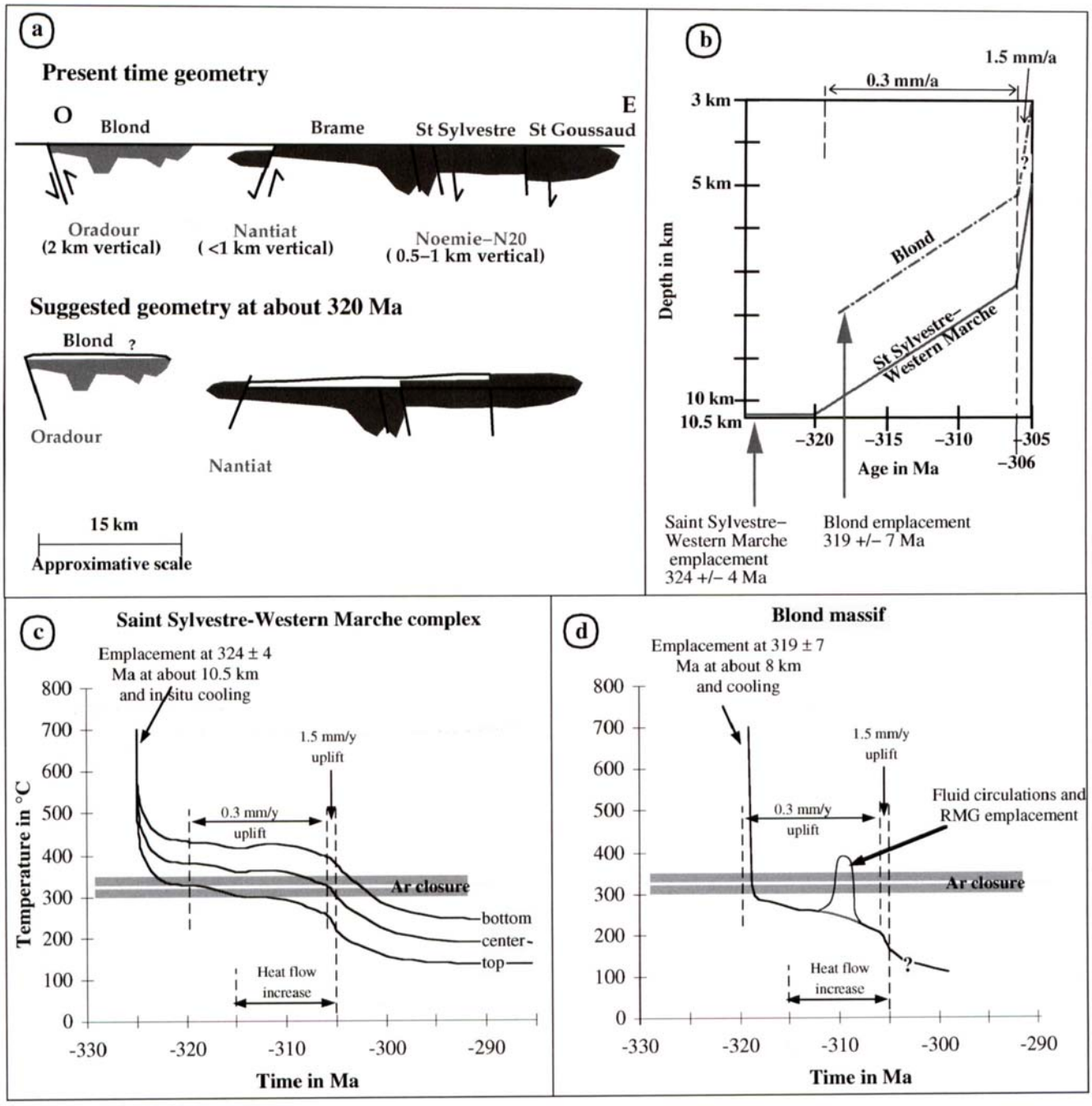

Figure 6 (a) Schematic reconstitution proposed at *c.* 320 Ma from the present time geometry and the structural data, on a W–E cross section; an emplacement depth of 8 ± 3 km is suggested for the Blond massif, based on the T–Z–t path proposed by Scaillet *et al.* (1996b), U/Pb dating (319 ± 7 Ma, Alexandrov *et al.* 2000) and present-time geometry; (b) comparison of Z–t paths of the Blond granite and the Saint Sylvestre complex; both paths are constrained by numerous data (Scaillet *et al.* 1996b; Alexandrov *et al.* 2000); however, the last part of the path of the Blond massif is mainly interpretative (analogy with the Saint Sylvestre path) due to the lack of data; (c) and (d) comparison of T–t evolution of the Blond granite and the Saint-Sylvestre complex; the shaded area corresponds to the Ar closure temperature interval (325 ± 25 °C) assumed by Scaillet *et al.* (1996a); according to Scaillet *et al.* (1996b), the Saint-Sylvestre complex was emplaced at a depth for which regional temperature was above the Ar closure temperature of muscovite; thus, Ar closure occurred during a cooling by exhumation, from 315 Ma to 300 Ma; in contrast, the Blond massif was emplaced at a depth for which regional temperature was below the Ar closure temperature of muscovite, leading to an almost immediate closure of Ar system in the granite; therefore, the observed $^{40}Ar/^{39}Ar$ ages (Alexandrov 2000) in the granite are interpreted as resulting from a reset of the Ar system induced by magmas and fluid transfers at *c.* 310 Ma.

Uranium was mainly held in low Th-uraninite, which is very easily leachable by oxidising fluid circulations. (ii) A second stage involved the brittle reactivation of these endogranitic shear zones, promoting intense circulation of meteoric fluids. This process led to a quartz leaching and alkali metasomatism of granite at 305 ± 1 Ma (Scaillet *et al.* 1996b), organised as a network of vertical conduits ('episyenites'). (iii) A final stage involved leaching of uranium by more superficial hydrothermal circulations (150–200 °C, 0·3–0·5 kbars) and its trapping in the episyenites or along brittle structures, in the 280–270 Ma interval (Leroy & Holliger 1984).

3.2 Relations between stream sediments, mineral occurrences and the structural model

The construction of the three-dimensional model permits comparison of the geological structures with mineral deposit occurrences and stream sediment geochemical maps. This comparison allows interpretation of the geometric and genetic relationships between granites and deposits (Be, Sn, W, Au and U) and related hydrothermal halos underlined by the regional distribution of these elements. These geochemical maps represent thirty chemical elements measured on approximately 11,000 data points (about 2 points/km^2), covering a large part of the studied area (see Figs 7 and 8). Because the stream sediment maps are computed by interpolation, only regional scale trends are considered. We first discuss those elements most closely related to granite outcrops.

Beryllium displays two interesting behaviours (Burnol 1974, Fig. 7b): (i) increasing concentration during magma fractionation; (ii) dispersed aureole above hidden intrusions suggesting the presence of concealed ore deposits. The abundance of Be in Guéret-type granites is generally low. However, the model shows that for several granite complexes or facies inside granite complexes, Be abundance is high. Interestingly, these zones also correspond to negative gravimetric anomalies. It is suggested that these areas reflect the more fractionated upper structural parts of Guéret-type complexes better preserved from erosion than elsewhere. In the upper structural parts of Guéret-type complexes, the density is close to that of Limousin-type granites, and thus explains the observed gravimetric anomalies, whereas in the lower structural parts, the density is close to that of surrounding rocks (Laurent 1989). Therefore, the three-dimensional model, where structural, geochemical and geophysical data may be displayed simultaneously, an a-priori model for density variations within granite complexes, may be proposed, and thus reduce the uncertainties of the gravimetric data inversions.

Most of the Limousin-type granites display regular and high Be abundance (Fig. 7b). Generally, the high Be abundances outline perfectly the structural outcropping boundaries of these leucogranites, and do not extend into the surrounding rocks, despite the separate origin of the data. Furthermore, no Be dispersion aureole is observed in the periphery of these granites, even in zones where the intrusion extends below surrounding rocks. For example, in the Saint Sylvestre complex, Be increases nearly continuously in each structural block toward the E, consistent with an increasing fractionation from the base to the top of the pluton (Burnol 1974). Inside this pluton, high-intensity anomalies occur. They are not specifically correlated with deeper zones, but with small albitic leucogranite cupolas and sodolithic pegmatites. In contrast, in the Blond granite area, Be shows a complex distribution within and outside the granite outcrop (Fig. 7b). A central depleted band is bordered to the N and to the S by two Be-rich bands, overlapping the granite outcrop and enclosing rocks. Several high-intensity Be anomalies are enclosed in these two bands. Some of them may correspond to Be-rich microgranites (Fig. 7b). Besides, the numerous small RMG intrusions occurring along the northern margin of the Blond massif could also explain some of these anomalies, as products of their highly fractionated chemical composition.

Tin in stream sediments (Fig. 8a) is located mainly inside granites, associated with Sn-rich facies of Limousin-type intrusions. In the Limousin, those correspond to uneconomic ore deposits.

In contrast, W stream sediment anomalies and ore deposit occurrences (Fig. 8b) are well correlated. They are mainly located in the metamorphic rocks, in the periphery of some of the Namurian Limousin-type granite massifs, the Auriat granite (Guéret-type) and in the vicinity of some leucogranitic bodies intruding the Guéret massif. The geometric model shows that these anomalies occur in particular close to the apex of Limousin-type granites, where they extend below enclosing rocks. However, these anomalies correspond to non-economic W deposits. The margins of the Blond massif and the Oradour fault are characterised by W stream sediment anomalies and subeconomic W deposits. These anomalies could be related to the presence of numerous RMG 'hidden cupolas' underneath the deposit; several examples are known in the close vicinity (Chèvremont *et al.* 1992; Cuney *et al.* 1999). This information highlights the particular role played by this kind of intrusion in the FMC (Marignac & Cuney 1999). However, although the Puy-les-Vignes W deposit displays a W anomaly similar to those related to the RMG, fluid inclusion data (see 3.1) and $^{40}Ar/^{39}Ar$ dating on a muscovite associated with the deposit (Alexandrov 2000) show that it was formed at a greater depth than the other deposits, and at *c.* 324 ± 1 Ma. This age, prior to any RMG intrusion (Marignac & Cuney 1999), indicates that in the Limousin at least two stages of W mineralisation occurred in the 325–310 Ma period (Alexandrov 2000).

Arsenic anomalies in stream sediment (corresponding to As > 80 ppm) represent the most interesting tracer to delineate the extension of palaeohydrothermal circulation, especially in relation with Au deposits (Bouchot *et al.* 1997, Figs 5 and 7a). Globally, the model shows that most diorites and Guéret-type granites do not present significant As anomalies. In contrast, these anomalies are geometrically correlated with Limousin-type granites. Two kinds of anomaly distribution may be distinguished (Fig. 7a).

(i) A low-intensity family occurs mainly in the LGU, to the E of Nantiat fault. These anomalies occur within a few kilometres around the most fractionated Limousin-type granites (for example the Saint Sylvestre and Saint Goussaud units). These anomalies correspond to the granite extension below the country rocks, as defined by the three-dimensional gravimetric data inversion (Fig. 7a); therefore, low intensity As anomalies are typically in apical configuration. Interestingly, the Auriat massif, belonging to Guéret-type but emplaced synchronously with Limousin-type granites, also has similar anomalies on its periphery. To a lesser extent, this kind of anomaly is also observed along the Arrènes–Ouzilly fault, over tens of kilometres.

(ii) A high-intensity family (Fig. 7a) occurs as isolated spots, which may be related to several W showings in the Guéret massif and to the Puy-les-Vignes W deposit. Elongated high-intensity As anomalies also occur along the Oradour fault and around the Blond massif, with an extension toward the N including the numerous RMG intrusion occurrences. The large As anomalies occurring indistinctly in both gneissic units as well as in the Guéret-type granites highlight the individuality of the Blond granite in the Limousin area, to be discussed later.

A similarity is observed between W and As anomalies, in terms of location as well as of intensity (Figs 5 and 7).

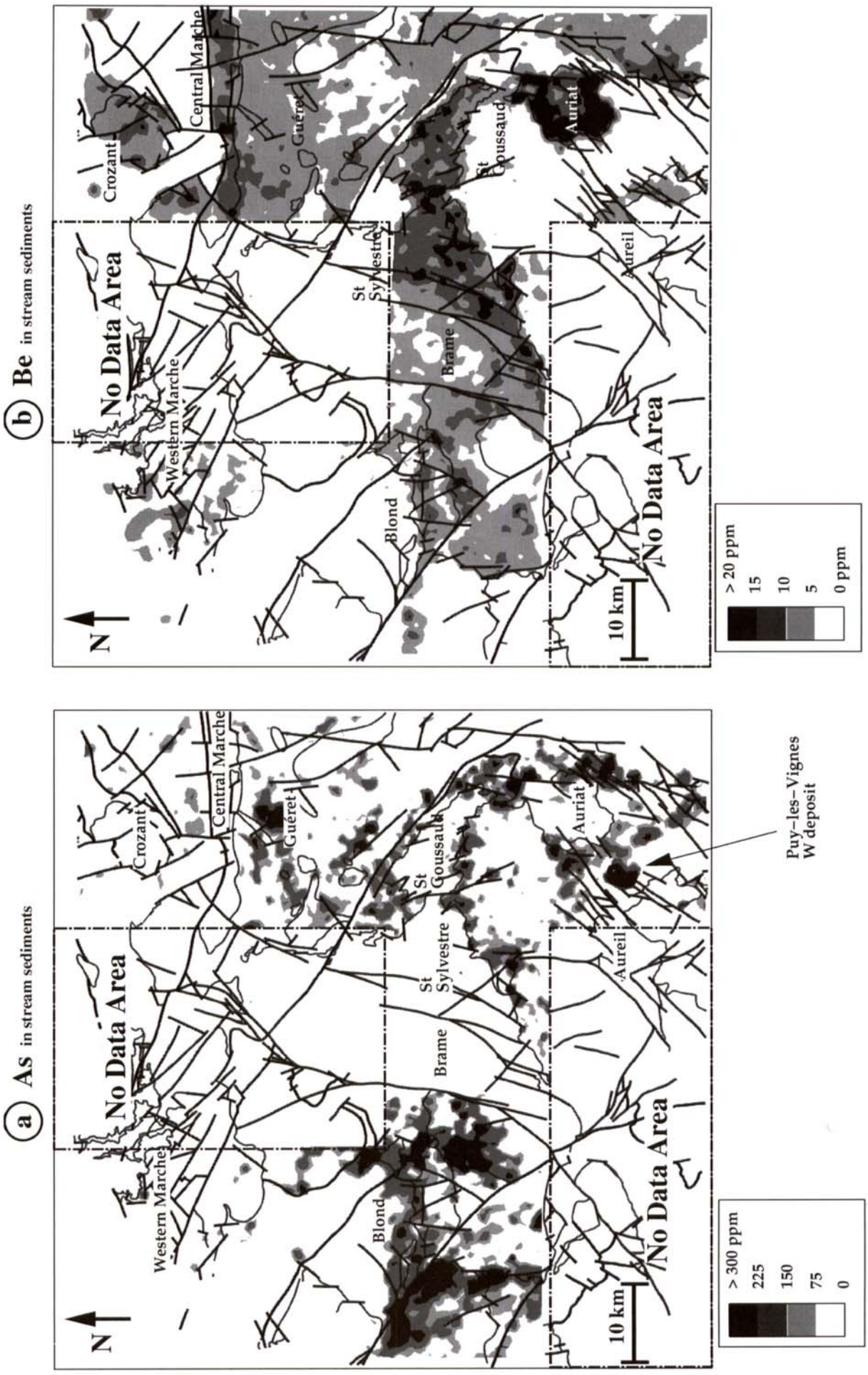

Figure 7 Geochemical stream sediment maps superimposed with a simplified surfacic geological map: (a) As anomalies (As > 80 ppm); (b) Be stream sediment map.

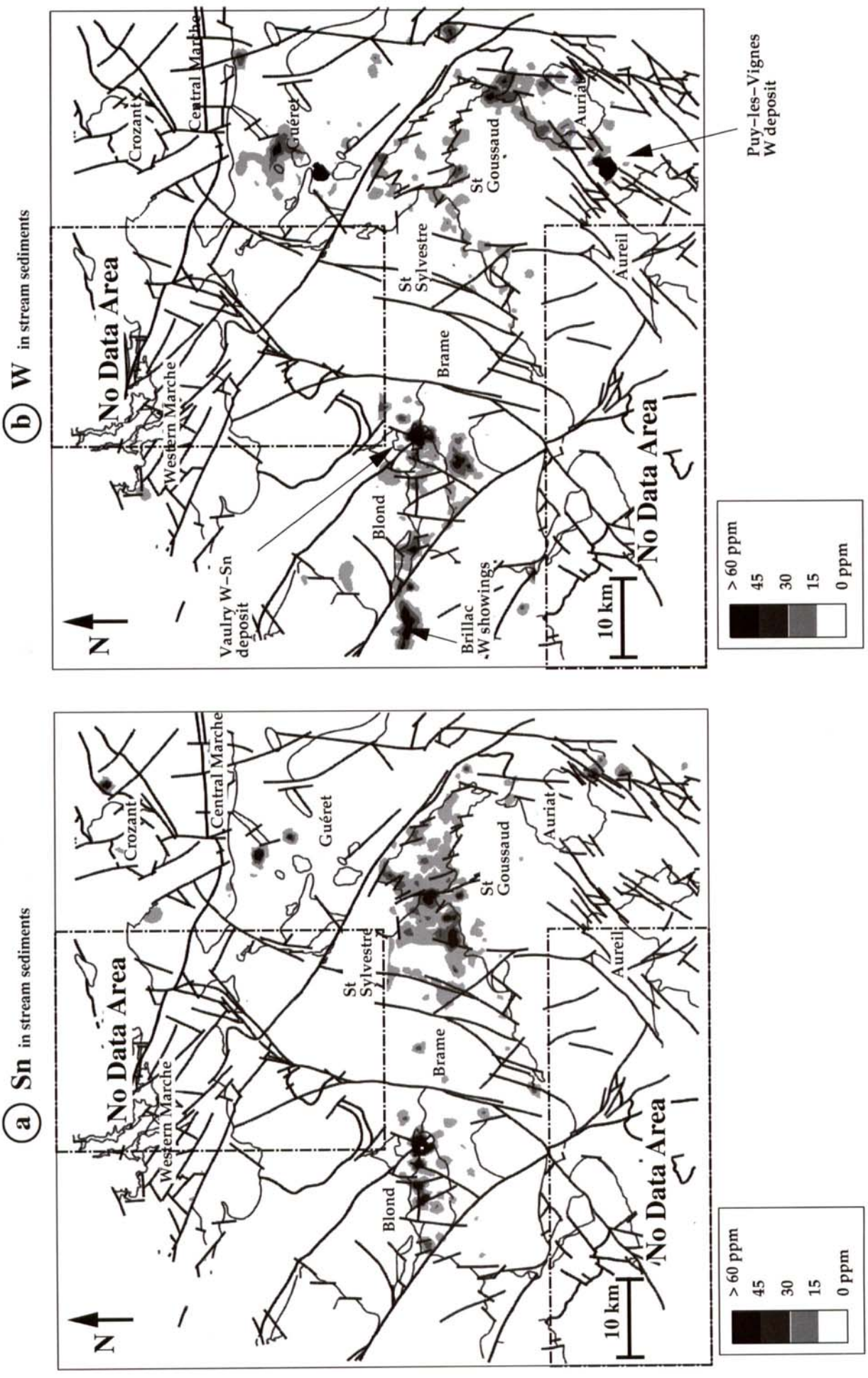

Figure 8 As Figure 7 with: (a) W stream sediment anomalies (W > 15 ppm); (b) Sn stream sediment anomalies (Sn > 25 ppm).

However, the W anomalies and deposits are mainly located close to the most apical part of Limousin-type or Rare Metal granite (Fig. 5), whereas As anomalies are more widespread and also located along some of the major shear zones, associated with some Au deposits. Consequently, W anomalies could be related to the fluid percolations limited to the vicinity of intrusions, whereas As anomalies reflect larger palaeocirculations inside permeable crustal zones.

Interestingly, As anomalies in stream sediments (Figs 5 and 7a) are not observed in the zone where U-bearing fluids are known to have percolated inside the granite massifs (Fig. 3), suggesting a difference in nature between U and Au-bearing fluids, as discussed by Dubessy *et al.* (1987) from thermodynamic data.

3.3 Limousin-type granite emplacement conditions

Previous results clearly highlight the spatial relationships between Limousin-type granites and ore deposits. It is also clear that each intrusion did not have the same effect on surrounding rocks and ore deposits. Thus, it is important to consider the conditions of emplacement of the different types of intrusion as well as their thermal impact. For that purpose, two- and three-dimensional modelling has been used, based on a reconstruction of the initial geometry of these massifs. The study was focused on the Saint Sylvestre complex and on the Blond massif, because of their relationship with numerous ore deposits and the large amount of data available on them (Scaillet *et al.* 1996a; Alexandrov 2000). In addition, similar kinds of recent isotopic dating (U/Pb and $^{40}Ar/^{39}Ar$) were available for both granites, reducing the discrepancies potentially introduced when comparing different dating methods. A transient conductive heat transfer model was used, assuming a single major intrusion. It provides an overestimation of the cooling time, because possible additional advective heat transfer would reduce it.

According to Scaillet *et al.* (1996b), the Saint Sylvestre complex was emplaced at about 324 ± 4 Ma (Holliger *et al.* 1986), as a 3 km-thick laccolith, and at an average depth of 10·5 ±1 km. The ductile–brittle transition was close to the roof of the laccolith, and corresponded to an average temperature of 350–400 °C. The numerical models showed that the cooling time duration for thermal equilibration with enclosing rocks was about 4 My.

At such depth, permeability of surrounding rocks was low and pressure conditions were lithostatic (Furlong *et al.* 1991). This was confirmed by fluid inclusions in quartz–arsenopyrite veins (Alikouss 1993) that record pressure and temperature conditions (2·5–3 kbar and 500 °C), consistent with the emplacement depth of the granite (10·5 ± 1 km) for lithostatic pressure conditions. Therefore, fluid circulation, occurring during the granite emplacement and its thermal equilibration with surrounding rocks mainly corresponds to prograde devolatilisation fluxes or retrograde fluid circulation from surrounding metamorphic rocks, induced by the intrusion heating. Fluid circulation occurs in the local and temporary fracture network in the vicinity of the granite (Furlong *et al.* 1991), as attested by the extent of As and W anomalies. However, these exchanges were limited in both time and space because: (i) the permeability of the surrounding rocks in ductile conditions was low (Furlong *et al.* 1991); and (ii) the tectonic regime has not allowed the development of a durable vertical high permeability zone at this period (Burg *et al.* 1994; Scaillet *et al.* 1996b). Consequently, the limited fluid circulation induced by the intrusion was disconnected from meteoric water infiltration (Furlong *et al.* 1991; Nesbitt & Muehlenbachs 1995).

Interestingly, a temperature, depth, time (T–Z–t) history of the Saint Sylvestre–Western Marche complex was proposed by Scaillet *et al.* (1996a, b; Fig. 6b, c), based on U/Pb and $^{40}Ar/^{39}Ar$ dating, numerical thermal modelling and fluid inclusion data. A two-stage uplift evolution was proposed (Fig. 6b): (i) the onset of post-collisional extension, characterised by a slow exhumation (0·3 mm/y) in the 320–300 Ma period followed by: (ii) a rapid uplift stage (1·5 mm/y), at *c.* 305 Ma. The early stages of the exhumation may correspond to the transition of the Saint Sylvestre laccolith from ductile to brittle conditions. The changes in tectonic conditions would have triggered fluid circulation along the fractures, leading to the formation of episyenites at *c.* 305 Ma. The 10–25 My separating the $^{40}Ar/^{39}Ar$ dating from the emplacement age of the complex has been explained as followed: (i) an emplacement and *in-situ* cooling at a depth for which the regional temperature was above the Ar closure temperature; and (ii) a cooling by exhumation, having led to Ar closure ages ranging from 315 Ma to 300 Ma, respectively from the top to the bottom of the complex.

The Blond granite was emplaced at 319 ± 7 Ma (U/Pb ion microprobe dating on zircons, Alexandrov *et al.* 2000). This massif is separated from the Saint Sylvestre complex (located 10 km to the E) by the Nantiat fault. The three-dimensional model was used to reconstruct its geometry at 319 Ma (Fig. 6a). Using the T–Z–t path proposed by Scaillet *et al.* (1996b) and assuming a 2 km vertical offset for the Nantiat fault, an estimated emplacement depth of 8 ± 3 km was proposed for the Blond massif (Fig. 6b). $^{40}Ar/^{39}Ar$ dating performed on muscovite indicates closure ages in the massif ranging from 312 to 306 Ma (Alexandrov 2000), but close to 338 ± 2 Ma for the surrounding metamorphic rocks. The ages observed in the surrounding rocks are interpreted as resulting from a regional cooling by exhumation at *c.* 340 Ma (Alexandrov 2000). However, the numerical three-dimensional models show that the maximum cooling time duration for thermal equilibration with surrounding rocks in these conditions is only *c.* 0·3 My. Thus, the muscovites of the granite should have closed their Ar isotopic system very rapidly, which is in disagreement with the $^{40}Ar/^{39}Ar$ dating in the granite. All muscovites in the granite present evidence of alteration, interpreted as resulting from later F-rich fluid hydrothermal circulations at a temperature above the muscovite closure temperature, taken at 325 ± 25 °C (Alexandrov 2000). Similarly, fluid inclusion studies (Vallance *et al.* 1999) on the Vaulry W–(Sn) deposit, dated by $^{40}Ar/^{39}Ar$ on hydrothermal muscovite at 309 ± 1 Ma (Alexandrov 2000), indicate formation conditions of 350–400 °C, under fluctuating pressure conditions ($\leqslant$ 1·2 kbars). The variability of the fluid inclusion temperature and composition has been interpreted by Cathelineau *et al.* (1999) as a mixing of fluids between magmatic or metamorphic fluids and downward percolating meteoric fluids.

In comparison with the Saint-Sylvestre massif, the Blond massif shows a more scattered distribution of Be and W in stream sediment and a larger extent of As anomalies in stream sediments. The previous dating (Alexandrov 2000) and fluid inclusion results (Vallance *et al.* 1999), show that significant circulations have occurred at a scale of several tens of kilometres around the Blond massif and the Oradour fault, at *c.* 310 Ma. This event was synchronous with the emplacement of multiple RMG bodies in this area (Cuney *et al.* 1999), and was probably related to the development of granulite-grade metamorphism in the lower crust (Marignac & Cuney 1999). According to the model of Scaillet *et al.* (1996b), at this time, the Blond area would have been at a depth of 4–6 km (Fig. 4b). Therefore, despite the slight overlap of dating uncertainties between U/Pb and $^{40}Ar/^{39}Ar$, it is

suggested that simultaneous Rare Metal intrusions and metamorphic or magmatic fluid circulations occurred in such shallow crustal level.

3.4 Regional tectonics and exhumation scenario

The distribution of the stream sediment anomalies clearly shows that the intrusion of Limousin-type and Rare Metal granites may have played a significant role especially for the Sn and W deposits, according to their emplacement conditions. However, taking into account the P, T, t, Z conditions of ore deposit formation and age determinations, the influence of granites in the other mineralisation processes (Au and U) does not appear as direct as is suggested by their tight spatial relationships. The time duration of the thermal perturbation induced by leucogranitic intrusions is much too small to explain the 30–50 My interval separating their emplacement from ore deposit formation. Furthermore, the previous paragraph showed the interest of setting back the evolution of these granites in the tectonic context.

Interestingly, a change in tectonic condition and exhumation rates, implying a two-stage exhumation, has been proposed by Scaillet *et al.* (1996b). The first stage of uplift with a low exhumation rate may correspond to the Late Visean–Westphalian (335–300 Ma), extension stage ('syn-convergence'), proposed by Burg *et al.* (1994) and Faure (1995). Incipient extension, occurring at the end of the continental convergence, is probably diachronous and concerns mainly the inner thickest parts of the belt. Wrench tectonics allows the lateral escape of crustal blocks. This stage is also characterised by the formation of Late Visean to Westphalian volcano-sedimentary basins (Bruguier *et al.* 1998). According to Burg *et al.* (1994), the syn-convergence extension stage does not imply a significant crustal thinning; however, it may explain the laccolithic shape of the leucogranites emplaced during this period (Faure & Pons 1991). In addition, the interaction between leucogranite emplacement and regional tectonics initiates a set of ductile faults, such as those allowing the relative downthrow of the Guéret massif. These faults have largely been reactivated later, in brittle conditions.

The second stage, with a high exhumation rate, corresponds to the gravitational collapse of the whole thickened domain that occurred from Late Stephanian to Autunian (300–280 Ma) (Burg *et al.* 1994). This stage implies a rapid thinning of the thickened crust, counterbalanced by an enlargement of the initial width of the belt. The increased uplift rate of 1·5 mm/y suggested by the numerical model at the beginning of the Stephanian cannot be produced by erosion only. It requires a contribution of tectonically aided denudation. This denudation can be achieved by detachment faulting, mainly focused along rheologically weak zones. inducing the exhumation of the ductile crust (Burg *et al.* 1994).

Therefore, we suggest that some of the main metallogenic events are related to a change in major tectonic regime in the 330–300 Ma period, from a compressional to an increasingly extensional regime. This major change was probably induced by lithospheric delamination (Pin 1989), as indicated by the thermal event necessary to explain the low pressure granulite-facies metamorphism of the lower crust (Pin & Vielzeuf 1983). The dehydration associated with the granulite-facies metamorphism of the lower crust produced F–Li–Sn–W–U rich fluids, which may have contributed to the genesis of the 'specialised' and Rare Metal granites (Cuney *et al.* 1990).

3.5 Implications for the mineralisation process

The previous results suggest that the onset of general extension during Late Stephanian to Autunian in the Variscan Belt (Burg *et al.* 1994) is a key factor controlling the metallogenesis in the Limousin area. On a regional scale, most of the resulting deposits are located in the vicinity of the ductile structures and granite; however, at the local scale, the relationships between deposits and these structures are not direct. In addition, large differences are observed in the stream sediments for the hydrothermal behaviour of Sn, W, Au and U. Consequently, this discussion focuses on the relationships between mineralisation, geological structures and tectonic regime, and will be divided in two parts: (i) synconvergence early extension (Visean–Westphalian, 335–310 Ma) and (ii) general extension and collapse of the belt (Westphalian–Permian, 310–280 Ma).

3.5.1. Synconvergence early extension. The Visean–Westphalian period is characterised by regional strike-slip ductile structures along which are emplaced Limousin-type granites. The exhumation rate for this period is low (Scaillet *et al.* 1996b; Burg *et al.* 1994).

The few low-grade Sn deposits occur inside Limousin-type granites, close to Sn-rich intrusions that suggest a major magmatic control through fractional crystallisation (Derré 1982) and limited hydrothermal circulations. Similarly, U preconcentration, already existing as uraninite in the $\gamma 1$ granite, was strongly enhanced during the intrusion of the later and more evolved $\gamma 2$ and $\gamma 3$ intrusions, in the Marche and Saint-Sylvestre complex (Fig. 3).

Tungsten (with minor tin) deposits are located in the vicinity of Limousin-type granite aureoles, especially in their upper structural part, in association with the most fractionated facies, which were also the richest in fluids. The close spatial and temporal association between W–(Sn) deposits and Limousin-type granites (Bouchot *et al.* 1999), and the high partition coefficient of W between fluid and melt, strongly suggest that the W source could be the leucogranites. However, none of these magmatic metal fractionations led directly to the formation of significant ore deposits, except for the Puy-les-Vignes W deposits, details of which were highlighted previously.

For Au deposits, the Visean–Westphalian period corresponds to the formation of quartz sulphide-arsenide bearing veins during ductile deformation. Gold veins are located along the ductile shear zones, such as Argentat and, to a lesser extent, the Oradour and Arrènes-Ouzilly ones. They also occur in the vicinity of Limousin-type granites, but at a greater distance than W–(Sn) deposits. All of them are associated with As anomalies of variable intensity. During this period, most of the currently outcropping granites and metamorphic rocks were under ductile to ductile-brittle conditions, at depths > 10 km. The global permeability of these rocks was low. In these conditions, the ductile shear zones, or fractured envelope around Limousin-type granites, represented zones with higher permeability where early magmatic/metamorphic fluids focused. A rather good estimation of the extent of associated hydrothermal systems is given by the distribution of As stream sediment anomalies that are related to the early fluid circulations (Cathelineau *et al.* 1990; Bouchot *et al.* 1989). For the Saint-Sylvestre complex, emplaced at a great depth ($10{\cdot}5 \pm 1$ km), these anomalies are only about 1–2 km in size (probably even less if the thickness is calculated perpendicularly to the granite contact), along the boundary of the complex.

Although almost no significant deposit seems to have occurred during this period, this stage is important from the metallogenic point of view for preparing favourable conditions for later fluid circulation, formation of metal preconcentrations and traps.

3.5.2. General extension. The Westphalian period is characterised by drastic changes in the tectonic regime with the onset of general extension, RMG emplacement and granulite-

facies metamorphism of the lower crust (Pin & Vielzeuf 1983), induced by the delamination of the lower lithosphere (Pin 1989). In the Limousin, extensional tectonics culminated during the Stephanian (at *c.* 305 Ma) with a transient fast tectonic denudation in the upper crust, leading to a large increase in the vertical permeability. This increase mainly occurred by reactivation of ductile structures, or of the thermally fractured aureoles induced by intrusion emplacement. These processes have led to a drastic pressure decrease and to the transition from lithostatic to hydrostatic regime. In addition, the exhumation of the ductile crust and the higher heat flow induced by the delamination of the lower lithosphere have both resulted in a transient uplift of the isotherms. For example, at *c.* 305 Ma, the Saint-Sylvestre Limousin-type complex is at an average temperature of 350 °C for an average depth of *c.* 5 km (Scaillet *et al.* 1996b; Fig. 6c). Therefore, during the 310–300 Ma period, this thermal anomaly, associated with an increase of the vertical permeability, has induced large fluid circulations, that have allowed the mixing of deep metamorphic fluids with meteoric and, subsequently, with basinal fluids.

Subeconomic W deposition occurred mainly during the intrusion of several RMG, especially in the Blond area, in the 310 ± 2 Ma period. Stream sediment distribution, $^{40}Ar/^{39}Ar$ dating (Alexandrov 2000) and fluid inclusion data (Vallance *et al.* 1999) provide further evidence of strong fluid and melt transfers at a kilometric scale in that area, which are coeval with the development of granulite-facies metamorphism in the lower crust. Therefore, it is suggested that simultaneous fluid and melt transfers occurring at shallow depths (*c.* 5 km), have induced buoyancy-driven fluid circulation (Furlong *et al.* 1991). This circulation has allowed a mixing between metamorphic-derived fluids and eventually late-magmatic fluids with meteoric fluids, and enhanced the W deposition. Interestingly, in the Saint-Sylvestre complex, the RMG intrusions also contributed to a strong U enrichment (Cuney *et al.* 1990);

For Au deposition, the Westphalian general extension and the associated fast exhumation rate control the brittle reactivation of former ductile structures (shear zones and to a lesser extent, fractured aureoles around Limousin-type granites). This reactivation allowed downward penetration of meteoric fluids (Cathelineau *et al.* 1990). The observed pressure drop (Bouchot *et al.* 1989) could be associated with the last extensional tectonic event and hydraulic fracturing. The LGU is the main host rock for Au deposits, but locally those ones occur in Guéret-type granites and in the UGU (Cathelineau *et al.* 1990). The LGU does not seem to have abnormally high gold concentrations, but it appears as a favourable host rock where trapping conditions were more efficient than in the other formations (Nénert et al. 1997).

In the Northern Limousin, the three-dimensional extent of the gold-bearing structures is unknown. However, in the gold mining district of Le Bourneix (southern Limousin, 20 km to the S of the modelled area, Bitri *et al.* 1999), two seismic profiles show that the mineralised structures may reach depths of more than 10 km. Therefore, Au mineralised structures have a real three-dimensional extension suggesting a very deep component in the Au mineralisation process.

In contrast to Au deposits, U deposits formed during Permian times are located well inside the leucogranites. In addition, at that time, most of the Limousin-type granites, such as the Saint-Sylvestre or Western Marche complexes, were uplifted to a brittle deformation structural level. During the fast exhumation, brittle fracturing led to the formation of vertical fractured zones inside the granites, reactivating older magmatic structures and petrologic discontinuities.

4. Conclusion

This work is a first step toward a three-dimensional reconstruction of the geological structures in the northern Limousin. Despite the limited amount of accurate data at depth, computer-aided three-dimensional modelling, that combines flexible tools for interpolating and editing objects in three-dimensions appears to be very efficient for creating geologically relevant models. Such modelling promotes the integration of all the geological data sets on a three-dimensional basis. It proposes a multilayer database, that may help in deciphering the interaction between magmatism, tectonics, thermal regime, fluid circulation and mineralisation. The integration of geophysical data is of first importance for imaging cryptic geometry, in relation to structural information. Combined with surfacic geochemistry (stream sediments and mineral occurrences), this multidisciplinary approach can investigate the impact of granitic intrusion, in relation to its geological context. In parallel, such impact may be quantified by numerical modelling, where the three-dimensional model is used to affect physical properties and to perform heat and mass transfers simulations. The results (time duration of the induced thermal perturbation, extent of the contact metamorphism) may thus be compared with available data. In the particular case of the northern Limousin, the three-dimensional model highlights the role played by the roof of Limousin-type granites, where fluid circulations were focused during the cooling of magmas.

Moreover, the current geometry also provides a reconstitution of the geometry at the time of the studied event. In parallel, numerical modelling provides P–T–Z–t paths constrained by the thermobarometric and geochronological data. Due to a limited amount of data, these paths are based on three-dimensional (vertical) time-dependant calculations, and the three-dimensional model is used to propose relevant geometrical simplification. However, and despite these simplifications, the models allow us to highlight differences between the evolution of granite complexes of the same typology, such as the Saint-Sylvestre and the Blond granite complexes (Fig. 6c, d).

The results of the modelling suggest that the location of the deposits, particularly those of Au and U, reflects the evolution of the vertical permeability of the crust during the 300 ± 30 Ma period, in response to the regional stress regime that prevailed during the same period. In the Northern Limousin, the 300 ± 30 Ma period corresponds to an evolution ranging from the beginning of the synconvergence extension and the associated magmatism (Visean), to the end of the general extension (Permian). For the early intrusions (360–320 Ma), emplaced in deep conditions (> 10 km), the low global permeability of surrounding rocks and the tectonic regime did not allowed vertical fluid exchanges to be established. Towards the end of the collision, the delamination of the lower lithosphere has probably played a major metallogenic role. Firstly, the emplacement of RMG, associated thermal anomalies and induced fracturing, occurring at a shallow depth (about 5 km) allowed the focus of fluids of different origins towards the apex of these plutons and led to the formation of significant W–Sn deposits. Secondly, the onset of general extension induced a rapid exhumation of the ductile crust, synchronously with the LP–HT granulite-grade metamorphism at the base of the crust. The resulting pressure decrease allowed increasing circulation of cool meteoric fluids and their mixing with deeper hot magmatic or meteoric fluids. The related fluid fluxes and the disequilibrium between fluids and surrounding rocks were of great importance for metal transportation and deposition within the reactivated permeable structures.

The change in the tectonic regime prevailing in the Variscan belt explains the several tens of million of years separating the formation of the ore deposits from the geographically associated Limousin-type granite intrusions. Although the culmination of ore deposit formation seems to have occurred during the 310 ± 5 Ma period, the ore deposit processes appear to be specific to each of the metals Sn, W, Au or U. For the W–Sn deposits related to RMG emplaced at *c.* 310 Ma, dating of mineralisations and of spatially associated intrusions indicates that they occurred almost simultaneously (Alexandrov 2000). A similar time interval is obtained in the Chataigneraie district (Cevennes region, 100 km to the S), concerning W deposits associated with leucogranites at *c.* 305 Ma (Lerouge *et al.* 1999; Bouchot *et al.* 1999). In contrast, for Au and U, the whole mineralisation process (including trap formation or preconcentration) involves several metallogenic steps, covering several tens of millions of years, and is controlled by the regional tectonic evolution of the Limousin area during the same period. Furthermore, some permeable zones seem have been used for different metal depositions. For example, the geographic correlation between early W–(Sn) and late Au–As deposits may indicate that the permeable fractured aureole around the granites was reactivated at least once. However, the thermodynamic conditions (T, fO_2, pH, nature and concentration of ligands) and the occurrence of adequate traps had the final control over the formation of significant ore bodies.

Finally, if three-dimensional modelling becomes increasingly important in addressing geological problems, more data, such as geophysical imaging of the crustal structures and systematic thermochronological dating of granite, but also of surrounding rocks, becomes necessary to refine the geological history of the Limousin crustal block. In addition, three-dimensional modelling of heat and mass transfers, constrained by combined fluid inclusion studies, win help in searching the sources of the fluids, their paths, and their effects on regional temperature field. These data could contribute to a better understanding of the complex evolution of the thermal regime and fluid circulation during the major metallogenic episode that took place in the Western European Variscan belt.

5. Acknowledgements

This work was supported by the GéoFrance 3D program '3D Mapping and Metallogeny of the French Massif Central', of which it is contribution number 82. The managers of this project, J.P. Milési and P. Ledru, are thanked for their help. CRPG contribution number 1441. The three referees (R. Seltmann and two anonymous referees) and the editor, B. Clarke, helped greatly in improving the manuscript. Ms Le Carlier is also thanked for her corrections.

6. References

Aissa, M., Weisbrod, A. & Marignac, C. 1987. Caractéristiques chimiques et thermodynamiques des circulations hydrothermales du site d'Echassières. *In* Cuney, M. & Autran, J. (eds) *Echassières: le forage scientifique. Une clé pour la compréhension des mécanismes magmatiques et hydrothermaux associés aux granites à métaux rares. Géologie de la France* **2–3**, 335–50.

Alikouss, S. 1993. Contribution à l'étude des fluides crustaux: approroche expérimentale et analytique (Unpublished PhD Thesis, INPL, Nancy).

Alexandrov, P. 2000. Géochronologie U/Pb et $^{40}Ar/^{39}Ar$ de deux segments Calédoniens et Hercyniens de la chaîne Varisque: Haut Limousin et Pyrénées Orientales (Unpublished PhD Thesis, INPL Nancy).

Alexandrov, P., Cheilletz, A., Deloule, E. & Cuney, M. 2000. 319 ± 7 Ma age for the Blond granite (northwest Limousin, French Massif Central) obtained by U/Pb ion-probe dating of zircons. *Académie des Sciences, Comptes Rendus* **330**, 1–7

Améglio, L., Vigneresse, J. L. & Bouchez, J. L. 1997. Granite pluton geometry and emplacement mode inferred from combined fabric and gravity data. *In* Bouchez, J. L., Button, D. H. W & Stephens, W. E. (eds) *Granite: From Segregation of Melt to Emplacement Fabrics* 199–214. Dordrecht: Kluwer.

Améglio, L., Cuney, M., Gagny, C. & Vigneresse, J. L. 1999. Shear-fault controlled emplacement of the Blond leucogranite (Limousin, France) inferred from geophysical and structural data. *EUG 10. Journal of Conference Abstracts* **4**. 1, 458, Cambridge Publications.

ASGA 1999. *gOcad User's Reference Manual.* ASGA, Nancy, France.

Audrain, J., Vigneresse, J. L., Cuney, M. & Friedrich, M. 1989. Modèle gravimétrique et mise en place du complexe granitique hyperalumineux de Saint-Sylvestre (Massif Central français). *Académie des Sciences, Comptes Rendus, Série II* **309**, 1907–14.

Autran, A. & Guillot, P. 1975. L'évolution orogénique et métamorphique du Limousin au Paléozoïque (Massif Central français). *Académie des Sciences, Comptes Rendus, Série D* **280**, 1649–52.

Barbier, J. 1967. Étude pétrographique et géochimique du granite à deux micas des Monts de Blond. *Sciences de la Terre, Nancy* **12**(3), 183–206.

Berthier, F., Duthou, J. L. & Roques, M. 1979. Datations géochronologiques Rb/Sr sur roches totales du granite de Guéret (Massif Central). Age fini-dévonien de mise en place de l'un de ses faciès type. *Bulletin du B.R.G.M; série II; section II* **2**, 59–72.

Bertrand, J. M., Leterrier, J., Delapierre, E., Brouand, M., Cuney, M., Stussi, J. M. & Virlojeux, D. 2001. Géochronologie U–Pb sur zircons de granitoïdes du Confolentais, du massif de Charroux-Civray (seuil du Poitou) et de Vendée. *Géologie de la France* (in press).

Bitri, A., Bouchot, V., Ledru, P., Milési, J. P., Bellot, J. P., Roig, J. Y. & Truffert, C. 1999. Deep seismic reflexion profile in Limousin region (French Massif Central). *Geophysical Research Abstracts, EGS'99. 24th General Assembly. Den Haag* **1**(1), 46.

Boiron, M. C., Cathelineau, M. & Trescases, J. J. 1989. Conditions of gold-bearing arsenopyrite crystallization in the Villeranges basin, Marche Combrailles shear zone, France: A mineralogical and fluid inclusion study. *Economic Geology* **84**, 1340–62.

Bouchot, V., Gros, Y. & Bonnemaison, M. 1989. Structural control on the auriferous shear zones of the St-Yrieix District, Massif Central, France: Evidence from the Le Bourneix and Laurieras gold deposits. *Economic Geology* **84**, 1315–27.

Bouchot, V., Milési, J. P., Lescuyer, J. L. & Ledru, P. 1997. Les minéralisations aurifères de la France dans leur cadre géologique autour de 300 Ma. *Chronique de la Recherche Minière* **528**, 13–62.

Bouchot, V., Alexandrov, P., Monié, P., Morillon, A. C., Cheilletz, A., Ruffet, G., Roig, J.Y., Charonnat, X., Chauvet, A., Faure, M., Le Carlier, C., Cuney, M., Becq-Giraudon, J. F., Truffert, C., Ledru, P. & Milési, J.P. 1999. The W–As–Au–Sb metalliferous peak: an 'instantaneous' marker of the late-orogenic evolution of the Variscan belt at 310–305 Ma. *In Colloque GéoFrance 3D: results and perspectives, Document BRGM* **293**, 33–6.

Bruguier, O., Becq-Giraudon, J. F., Bosch, D. & Lancelot, J. 1998. Late Visean (Upper Mississippian) Hidden Basin in the Internal Zones of the Variscan Belt: U–Pb Zircon Evidence from the French Massif Central. *Geology* **26**, 627–30.

Burg J. P., Van Den Driessche J. & Brun J . P. 1994. Syn- to post-thickening extension: mode and consequences. *Académie des Sciences, Comptes Rendus, Série II* **319**, 1019–32.

Burnol, L.1974. Géochimie du béryllium et types de concentration dans les leucogranites du Massif Central français. *Mémoires du BRGM* **85**.

Cathelineau, M., Boiron, M. C., Holliger, P. & Poty, B. 1990. Metallogenesis in the French part of the Variscan orogen. Part II: Time-space relationships between U, Au and Sn–W ore deposition and geodynamic events – mineralogical and U–Pb data. *Tectonophysics* **177**, 59–79.

Cathelineau, M., Marignac, C., Fourcade, S., Cuney, M., André, A. S., Boiron, M. C., Chauvet, A., Charonnat, X., Lespinasse, M., Martineau, F., Menez, B., Nomade, S., Philippot, P., Souhassou, M., Vallance, J. & Milési, J. P. 1999. Sources of fluids and regimes of fluids during the Late Carboniferous uplift of the Variscan crust and consequences on metal transfer and deposition. *In Colloque GéoFrance 3D: results and perspectives, Document BRGM* **293**, 46–8.

Chèvremont, P., Constans, J., Ledru, P. & Ménillet, F. 1992. Booklet of the 1/50,000th geological map of Oradour. BRGM.

Cuney, M., Friedrich, M., Blumenfeld, P., Bourguignon, A., Boiron, M. C., Vigneresse, J. L. & Poty, B. 1990. Metallogenesis in the French part of the Variscan orogen. Part I: U preconcentration in pre-Variscan and Variscan formations – a comparison with Sn, W and Au. *Tectonophysics* **177**, 39–57.

Cuney, M., Stussi, J.M. & Marignac, C. 1994. A geochemical comparison between west- and central European granites: implications for the origin of rare metal mineralisations. *In* Seltmann, R., Kämpf, H. & Möller, P. (eds) *Metallogeny of collisional orogens* 96–102. Prague: Czech Geological Survey.

Cuney, M., Pin, C. Raimbault, L. & Gagny, C. 1999. Magmatic fractionation and geochemical exchange with enclosing rocks in F, Li, P and rare metal enriched microgranite dykes, a three dimension approach. *In* Barbarin, B. (ed.) *The origin of granite and related rocks, Fourth Hutton Symposium Abstracts, Document du BRGM* **290**, 231.

Cuney, M. & Stussi, J. M. 1999. The origins of the two main types of Variscan peraluminous granites from the French Massif Central. *In* Barbarin, B. (ed.) *The origin of granites and related rocks – Abstracts of the 4th Hutton Symposium. Document du BRGM* **290**, 207. Clermont-Ferrand: BRGM.

Derré, C. 1982. Caractéristiques de la distribution des gisements à etain et tungstène dans l'ouest de l'Europe. *Mineralium Deposita* **17**, 55–77.

Dubessy, J., Ramboz, C., Nguyen-Trung, C., Cathelineau, M., Charoy, B., Cuney, M., Leroy, J., Poty , B. & Weisbrod, A. 1987. Physical and chemical controls (fO_2, T , pH) of the opposite behaviour of U and Sn–W as exemplified by hydrothermal deposits in France and Great Britain, and solubility data. *Bulletin Minéralogique* **110**, 261–81.

Dumas, E., Faure, M. & Pons J. 1990. L'architecture des plutons leucogranitiques du plateau d'Aigurande et l'amincissement crustal tardi-varisque. *Académie des Sciences, Comptes Rendus, Série II*, **310**, 1533–9.

Duthou, J. 1978. Les granitoïdes du Haut Limousin (Massif Central français) chronologie Rb/Sr de leur mise en place; le thermométamorphisme carbonifère. *Bulletin de la Société Géologique de France, (7)*, **20**, 229–35.

Duthou, J., Cantagrel, J. M., Didier, J. & Vialette, Y. 1984. Paleozoic granitoids from the French Massif Central: age and origin studied by the ^{87}Rb–^{87}Sr system. *Physics of the Earth and Planetary Interiors* **35**, 131–44.

Eisenlohr, B., Groves, D. & Partington, G. 1989. Crustal-scale shear zones and their significance to Archaean gold mineralization in Western Australia. *Economic Geology* **24**, 1–8.

Faure, M. & Pons, J. 1991. Crustal thinning recorded by the shape of Namurian–Westphalian leucogranite in the Variscan belt of the northern Massif Central, France. *Geology* **19**, 730–3.

Faure, M. 1995. Late orogenic Carboniferous extensions in the Variscan French Massif Central. *Tectonics* **19**, 132–53.

Furlong, K. P., Hanson, R. B. & Bowers, J. R. 1991. Modelling thermal regimes. *In* Kerrick, D. M. (ed.) *Contact metamorphism, Reviews in Mineralogy* **26**, 437–505.

Gebauer, H., Bernard-Griffiths, J. & Grünenfelder, M. 1981. U/Pb zircon and monazite dating of mafic-ultramafic complex and its country rocks. Example: Sauviat-sur-Vige, French Massif Central. *Contributions to Mineralogy and Petrology* **76**, 292–300.

Gérard, B. 1997. Modélisation 3D des transferts de chaleur et de fluide dans les formations sédimentaires. Application aux réacteurs d'Oklo (Gabon) (Unpublished Ph.D. Thesis, INPL, Nancy).

Guineberteau, B., Cuney, M. & Carre, J.L. 1989. Structure magmatique et plastique des granites de la Marche occidentale: un couloir transformant hercynien dans le NW du Massif Central Français. *Académie des Sciences, Comptes Rendus, Série II* **309**, 1695–702.

Holliger, P., Cuney, M., Friedrich, M. & Turpin, L. 1986. Ages carbonifères de l'unité de Brame du complexe granitique peralumineux de Saint Sylvestre (NO Massif Central) défini par les données isotopiques sur zircon et monazite. *Académie des Sciences, Comptes Rendus, Série II* **303**, 1309–14.

Laurent, O. 1989. Le sondage de Créchat-les-Sibieux, apports à la connaissance géologique de l'ouest du Massif Central français (Unpublished Ph.D. Thesis, Université Pierre et Marie Curie, Paris).

Ledru, P., Lardeaux, J. M., Santallier, D., Autran, A., Quénardel, J. M., Floc'h, J.P., Lerouge, G., Maillet, N., Marchand, I. & Ploquin, A. 1989. Où sont passées les nappes dans le Massif Central français? *Bulletin de la Société Géologique de France* **8**, 605–18.

Lerouge, C., Fouillac, A. M., Roig, J. Y. & Bouchot, V. 1999. Stable isotope constraints on the formation temperature and origins of the Late Variscan As–W mineralization at La Chataigneraie, Massif Central, France. *EUG 10. Journal of Conference Abstracts* **4**, 1, 483, Cambridge Publications.

Leroy, J. & Holliger, P. 1984. Mineralogical, chemical and isotopic (U–Pb method) studies of the Hercynian uraniferous mineralizations (Fanay and Margnac mines, Limousin, France). *Chemical Geology* **45**, 121–34.

Lespinasse, M., Mollier, B., Delair, I. & Bladier, Y. 1986. Structuration tangentielle et chevauchements carbonifères dans les leucogranites du NW du Massif Central français: l'exemple des failles de Bussière-Madeleine et d'Arrênes-Ouzilly. *Académie des Sciences, Comptes Rendus, Série II* **303**, 1575–80.

Mallet, J. L. 1992. Discrete smooth interpolation. *Computer-aided design* **24**(4), 178–91.

Mallet, J. L. 1997. Discrete modelling for natural objects. *Mathematical Geology* **29**, 199–219.

Marignac, C. & Cuney, M. 1999. Ore deposits of the French Massif Central: insight into the metallogenesis of the Variscan collision belt. *Mineralium Deposita* **34**, 472–504.

Nenert, S., Bril, H. & Floc'h, J. P. 1997. Les districts aurifères du Haut-Limousin Massif Central français: approche minéralogique et géochimique. *Chronique de la Recherche Minière* **526**, 3–15.

Nesbitt, B. & Muehlenbachs, K. 1995. Geochemical studies of the origins and effects of synorogenic crustal fluids in the southern Omineca Belt of British Columbia, Canada. *Geological Society of America Bulletin* **107**,1033–50.

Peiffer, M. T. 1986. La signification de la ligne tonalitique du Limousin. Son implication dans la structuration varisque du Massif Central français. *Académie des Sciences, Comptes Rendus, Série II* **303**, 305–10.

Pin, C. 1989. Essai sur la chronologie et l'évolution de la géodynamique de la chaîne hercynienne d'Europe (Doct. Sci. Thesis, Université Clermont-Ferrand).

Pin, C. & Vielzeuf, D. 1983. Granulites and related rocks in Variscan median Europe: A dualistic interpretation. *Tectonophysics* **93**, 47–74.

Pollard, P. J. 1989. Geochemistry of granites associated with tantalum and niobium mineralisation. *In* Möller, P., Cerny, P. & Saupé, F. (eds) *Lanthanides, tantalum and niobium*, 27–9. Berlin: Springer.

Raimbault, L. 1998. Minéralisations Sn–W et granites à métaux rares en Nord-Limousin. Zonalité géochimique du prospect de Moulin Barret et du massif granitique de Blond. *Rapport LHM/RD/98/56, GéoFrance 3D project.*

Roig, J. Y. & Faure, M. 2000. La tectonique cisaillante polyphasée du Sud Limousin (Massif Central français) et son interprétation dans un modèle d'évolution polycyclique de la chaîne hercynienne. *Bulletin de la Société Géologique de France* **171**, 295–307.

Rolin, P. & Quénardel, J. M. 1982. Modèle de mise en place syntectonique d'un massif de leucogranite hercynien (Crozant, NW du Massif Central français). *Académie des Sciences, Comptes Rendus, Série II*, **294**, 799–802.

Scaillet, S., Cheilletz, A., Cuney, M., Farrar, E. & Archibald, A. D. 1996a. Cooling pattern and mineralisation history of the Saint-Sylvestre and Western Marche leucogranite pluton, French Massif Central: I. $^{40}Ar/^{39}Ar$ isotopic constraints. *Geochimica et Cosmochimica Acta* **60**(23), 4653–71.

Scaillet, S., Cuney, M., Le Carlier de Veslud, C., Cheilletz, A. & Royer, J. J. 1996b. Cooling pattern and mineralisation history of the Saint Sylvestre and Western Marche leucogranite pluton, French Massif Central: II. Thermal modelling and implications for the mechanisms of U-mineralization. *Geochimica et Cosmochimica Acta* **60**(23), 4673–88.

Stussi, J. M. 1985. Magmatic control of granite related mineralizations in the French Variscan. *Fortschritt in Mineralogie* **63**, 229.

Stussi, J. M. & Cuney, M. 1993. Modéles d'évolution géochimique de granitoïdes paralumineux. L'exemple du complexe plutonique varisque du Millevaches (Massif central français). *Bulletin de la Société Géologique de France* **164**, 585–96.

Touray, J. C., Marcoux, E., Hubert, P. & Proust, D. 1989. Hydrothermal process and ore forming fluids in the Le Bourneix gold deposit, central France. *Economic Geology* **84**, 1328–39.

Turpin, L., Cuney, M., Friedrich, M., Bouchez, J. L. & Aubertin M. 1990a. Meta-igneous origin of Hercynian peraluminous granites in N.W. French Massif Central; implication for crustal history reconstitutions. *Contributions to Mineralogy and Petrology* **104**, 163–72.

Turpin, L., Leroy, I. & Sheppard, S. 1990b. Isotopic systematics (O, H, C, Sr, Nd) of superimposed barren and U-bearing hydrothermal systems in a Hercynian granite, Massif Central, France. *Chemical Geology*, **88**, 85–98.

Vallance, J., Boiron, M. C., Fourcade, S., Cathelineau, M. & Marignac, C. 1999. Fluid migration in granites associated with W–Sn–(Au) ores; The example of the Vaulry deposit in the Blond Rare Metal Granite (NW French Massif Central). EUG 10, *Journal of Conference Abstracts* **4**, 1, 478. Cambridge Publications.

Vasseur, G., Dupis, A., Gallart, I. & Robin, G. 1990. Données géophysiques sur la structure du massif leucogranitique du Limousin. *Bulletin de la Société Géologique de France* **1**, t.VI, 3–11.

Vigneresse, J. L. & Cuney, M. 1994. The Western Marche granite, France. *In* Haslam, W. *et al.* (eds) *Granite, metallogeny, lineaments and rock-fluid interactions. British Geological Survey Research Report SP/94/1*, 54–9. Keyworth: BGS.

Virlogeux, D., Roux, J. & Guillemot, D. 1999. Apport de la géophysique à la connaissance du massif de Charroux-Civray et du socle poitevin. *In Etudes du Massif de Charroux-Civray, Actes des journées scientifiques CNRS-ANDRA, EDP sciences, Les Ulis*, 33–62.

C. Le CARLIER de VESLUD, J. J. ROYER and P. ALEXANDROV, CRPG-CNRS & LIAD-ENSG, Rue du Doyen Marcel Roubault BP 40, 54 500 Vandoeuvre-lès-Nancy, France
M. CUNEY and J. L. VIGNERESSE, UMR 7566 G2R-CREGU, BP 239, 54506, Vandoeuvre-lès-Nancy, France
J. P. FLOC'H, Facultés des Sciences, Laboratoire de Géologie Structurale et Hydrothermalisme, 123 Av. A. Thomas, 87060 Limoges, France
L. AMÉGLIO, Rhodes University, Geology Department, P.O. Box 94, Grahamstown 6140, South Africa
P. CHÈVREMONT and Y. ITARD, BRGM, SNG-CMG-GEO, BP 6009, 45060 Orléans cedex 2, France

MS received 15 December 1999. Accepted for publication 14 August 2000.